

## Point-by-Point reply to the comments

We thank the editor and both anonymous referees for their constructive comments. We have addressed all of them in the following point-to-point rebuttal letter and we incorporated the changes in a revised manuscript. Specifically, we have strengthened the case for the presence of an active sinkhole in Pieve Fosciana by adding a geomorphological and structural map, a geological cross-section and a stratigraphic log from borehole data. Furthermore, we expanded the seismicity analysis and added a figure clearly showing lack of correlation between distant earthquakes and sinkhole unrest. We also included a description of a recent geochemical study showing that fluids at Prà di Lama migrate along faults from a carbonatic reservoir at 2 km depth. We believe that the additional evidences show to greater confidence that the Prà di Lama lake is a sinkhole whose formation and growth is linked to the local active tectonics.

As comments by the reviewers have some common themes, we have sorted each reviewer's comments and grouped those that have common themes.

### # Editor

Major revisions are required to the manuscript, in order to consider it for publication. In addition to the comments by the referees, I suggest the Authors to refer to internationally recognized classification on sinkholes, such as that proposed in Gutierrez et al. (2008, 2014) rather than referencing to single publications. This will help the reader to have a better understanding of the processes authors are describing.

Further, Authors do not take into any account a number of papers dealing exactly with the topic of the manuscript, that is the relations between sinkhole and seismicity. I kindly invite the Authors to consider such references when preparing the revised version of the manuscript. Below Authors will find a list of suggested references:

Del Prete, S., Iovine, G., Parise, M., Santo, A., 2010b. Origin and distribution of different types of sinkholes in the plain areas of Southern Italy. *Geodin. Acta* 23, 113–127.

Gutiérrez, F., Guerrero, J., Lucha, P., 2008. A genetic classification of sinkholes illustrated from evaporite paleokarst exposures in Spain. *Environ. Geol.* 53, 993–1006.

Gutierrez F., Parise M., De Waele J. & Jourde H., 2014, A review on natural and human-induced geohazards and impacts in karst. *Earth Science Reviews*, vol. 138, p. 61-88, doi: 10.1016/j.earscirev.2014.08.002.

Iovine G. & Parise M., 2008, I sinkholes in Calabria. In: Nisio S. (a cura di) I fenomeni naturali di sinkhole nelle aree di pianura italiane. *Memorie Descrittive della Carta Geologica d'Italia*, vol. 85, p. 335-386.

Kawashima, K., Aydan, O., Aoki, T., Kishimoto, I., Konagal, K., Matsui, T., Sakuta, J., Takahashi, N., Teodori, S.-P., Yashima, A., 2010. Reconnaissance investigation on the damage of the 2009 L'Aquila, Central Italy earthquake. *J. Earthq. Eng.* 14, 817–841.

Parise, M., Perrone, A., Violante, C., Stewart, J.P., Simonelli, A., Guzzetti, F., 2010. Activity of the Italian National Research Council in the aftermath of the 6 April 2009 Abruzzo earthquake: the Sinizzo Lake case study. *Proc. 2nd Int. Workshop "Sinkholes in the Natural and Anthropogenic Environment"*, Rome, pp. 623–641.

Santo, A., Del Prete, S., Di Crescenzo, G., Rotella, M., 2007. Karst processes and slope instability: some investigations in the carbonate Apennine of Campania (southern Italy). In: Parise, M., Gunn, J. (Eds.), *Natural and Anthropogenic Hazards in Karst Areas: Recognition, Analysis, and Mitigation*. Geological Society, London. 279, pp. 59–72.

**Response:** We modified our manuscript as suggested. We now use in our manuscript the international classification of sinkholes proposed by *Gutierrez et al. (2008, 2014)* see changes to the text at lines 29-35 and 289-291. We also improve the description of seismically induced sinkholes in Italy by referring to all the suggested papers in the discussion section, see changes at lines 50-54.

### # Reviewer 1.

- the few number of independent sources (SBAS, historical data, field survey, and seismic analysis);
- their variable quality levels (field observations not enough extended);
- their limited nature (there is no geomorphological map, no structural map, no trenching, no SBAS field validations, no sub-surface geophysics, no boreholes);
- structural map is not presented while this source of data is interesting to link the genesis of the depression with a possible seismic creep;
- geomorphological maps, at local and regional scales, should be drawn in order to confirm that this depression is really a singularity in the landscape. There is no evidence anywhere that this depression is an isolate case or that similar phenomena can be observe elsewhere in the region. It is really important to clarify the status of this de-pression because if it is an isolated case, then, it can be considered a very interesting indicator regarding the tectonic activity in the region;
- the stratigraphy is very poorly described and the thickness of the different layers below the depression is incomplete. A carbonate layer is mentioned in the text (Tuscan Nappe Unit) but not its depth while this layer is a good candidate to be the siege of dissolution phenomena leading to ground subsidence at the surface.

### # Reviewer 2, specific comment 2.1:

The paper lacks essential data on the geomorphic context, including a detailed map. The latter may show the presence of landslides or other sinkholes in the area. A thorough geomorphological analysis is needed to identify the active processes in the study area and distinguish their relative importance in the sinkhole deformation dynamic. Such as: detailed mapping, trenching combined with geochronological data (to study the geological record and increase the temporal registry), and geophysics.

**Response:** We agree with the reviewers that a better description of the stratigraphy, geology, tectonic structures, and geomorphology of the Pieve Fosciana area is needed to improve the paper, providing more compelling evidences of the presence of an active sinkhole and its relationship to tectonics. Therefore, we added a geomorphological and structural map (Fig. 2a) as well as a geological cross-section of the study area (Fig. 2c). The latter shows the stratigraphy of the Prà di Lama sinkhole and the presence, at ~ 2 km depth, of carbonatic and evaporitic formations. The geomorphological map also shows the presence of the Prà di Lama sinkhole and the lack of landslides in the area affected by ground motion as identified by InSAR. The Prà di Lama sinkhole is an isolated feature in the region being the only mapped sinkhole in the entire Garfagnana graben (*Caramanna et al., 2008*); the closest sinkholes are near the Tuscany coast. We added to figure 1 the locations of the sinkholes to clearly show the Prà di Lama site is an isolated case. We also expanded on the field observations by adding photos of fractures and cracks around the lake that further document the deformation activity at Prà di Lama (Supp. Fig. 1 and Suppl. Fig. 2). Observations from a 200 m-deep borehole have been also added, showing the detailed stratigraphy (Fig. 2b). A recent study from *Gherardi and Pierotti (2018)*, expanding on previous research (*Baldacci et al., 2007*), uses geo-chemical analyses of the Prà di Lama spring waters and concludes that the high salinity (~5.9g/kgw) and temperature (~57 °C) are explained by hydrothermal circulation be-tween 1.3 and 2 km depth in an evaporitic-carbonate reservoir. The results from this study are in agreement with the presence of a deep sinkhole at Prà di Lama, and the evaporitic-carbonate reservoir likely corresponds to the anhydrite of the Burano Fm. and the calcareous-dolomitic breccia of the Calcare Cavernoso Fm., as shown by our geologic cross-section Fig. 2c). More importantly, the un-mixing of deep waters in shallow aquifers is interpreted by *Gherardi and Pierotti (2018)* as an evidence of the rapid upwelling of deep waters along the main tectonic structures (*Baldacci et al., 2007*). The conclusions reached by the authors have been added to the manuscript in the discussion section. Our revised dataset now includes observations from completely independent methods spanning surface deformation (InSAR), structural geology, seismicity,

geomorphology, borehole stratigraphy and a century-long historical record of sinkhole activity. We now also include a comparison of our results to independent geochemistry results. Several independent lines of evidence that support our conclusions are now provided. Data from subsurface geophysics and trenching in Pieve Fosciana are not available and their high cost prevents us to obtain these datasets at present. While these data provide a more detailed view of the source geometry and fault activity, we believe that the main conclusions reached by our study are still supported and our dataset adds new and relevant information to the debate about sinkhole formation and their link to active tectonic structures. We hope that our study will raise the scientific interest in the area and that subsurface geophysics and trenching will be carried out in the future.

#### # Reviewer 1.

- Partial temporal and spatial overlap. (most information are concentrated in the last two decades);
- The historical record is a too limited set of observations. They are informative but could become much more relevant if they were complemented by trenching and dating as it is done in paleo-seismology in combination with historical data does not allow a clear understanding of the sinkhole formation. The idea of seismic creep seems to me not supported by a robust analysis performed at local and regional scales. The sub-surface geophysical facet is missing and therefore it is very difficult to be convinced with this explanation. Much deeper investigations are still needed.

**Response:** The first information about the Prà di Lama lake date back to the 991 A.D., when it was reported that a depression filled by a lake formed from a series of previously isolated springs. We added this explanation to the manuscript to clarify that the historical record allows us to define the time-scale of sinkhole formation. Furthermore, the historical record shows well the episodic behaviour of the sinkhole; this has also been clarified in the manuscript. We agree with the reviewer that the historical record is limited and therefore we complemented it with InSAR, seismicity and structural geology data that have now been expanded to include geomorphology, borehole stratigraphy and a comparison to a recently published geochemistry study. See also our previous response. Regarding the seismicity analysis, we used a reputed catalogue, the Italian national catalogue of seismicity recorded by the *Istituto Nazionale di Geofisica e Vulcanologia (INGV)* and available online (<http://cnt.rm.ingv.it/search>). We already analysed the seismic moment release and magnitude contents both in the broader tectonic region and at the local scale. The complete dataset containing all the low magnitude events ( $M_l < 2.0$ ) dates back to the 1986. Other historical catalogue exists, but earthquakes locations are not accurate, nor are the magnitudes. This makes it difficult to attribute an earthquake to one of the faults nearby the lake. Thus, we decided to limit our analysis to seismic data from 1986 and we clarified this in the manuscript. To strengthen our tectonic interpretation, we expanded the section on fault creep providing examples where a comparable fault activity has been suggested. We have shown examples from Taiwan (*Rau et al., 2007; Chen et al., 2008; Harris, 2017*) and Parkfield (California) (*Nadeau et al., 1995, Harris, 2017*). InSAR is a fairly recent technique and we do not have data past the last few decades thus we have complemented our observations of recent subsidence to structural geology providing stronger evidences of the longer-term tectonic activity in the area. We added a more detailed structural geology map showing the faults in the area.

**Comment:** The authors are performing some comparisons with the Dead Sea sink-holes. In Israel, lot of geophysical studies have been performed in the last 15 years to create a robust model combining geomorphological mapping, structural inputs, InSAR ground deformations and shallow geophysical study results (e.g. Ezersky et al.). In this paper, most of the data are not sufficient to quantify/to observe a possible link between seismic creep and the dynamic of the collapsed area. Aware of the literature regarding the Dead Sea sinkholes, I would like to point out the attention of the authors on a circular

depression located in the Jordanian Dead Sea zone and named "Birkat El Haj". It is described as a salt collapse structure. A priori, it seems to me that a comparison in term of genesis could be established.

**Response:** We added to our discussion section the example of the Birkat El Haj sinkhole as suggested.

**Comment:** the authors described the depression as a circular feature. However, the analysis of the contours indicates that the depression is more elliptical than circular. The lowest elevations (lake) are not located in the centre of the ellipse but rather in the SW side. This asymmetry and the cracks mapped during the field survey suggest a gradual migration SW wards from the original collapse. Is this SW-NE direction important with regard to the structural data in the region? If validated, this interpretation would mean that trenches could be excavated in the NE part of the depression to potentially reveal former shorelines of the lake

**Response:** The temporal reconstruction shows that the lake had a quasi-circular shape between 1994 and 2014. The events of 1996, in fact, consisted in a lake-level fluctuation accompanied by slumping of the shores and cracks formation (yellow lines in Fig. 3 and Supp. Fig. 1). No significant changes in the lake's shape or dimension occurred in 1996. The elliptical shape results from the last event of 2016. During that event fracture formed in the SW as a consequence of subsidence. The main active strike-slip fault is also oriented SW, suggesting a tectonic control on the deformation and in agreement with our interpretation of tectonic-induced sinkhole. This explanation has been added to the manuscript. Figure 3 has also been modified as requested and a structural map (Fig 2a) has been added in our manuscript together with photos (Supp. Fig. 1 and Supp. Fig. 2) that better document the most recent phenomena.

**Comment:** The SBAS analysis presents interesting results but the reference point is not indicated. Besides, what is the stability of the reference point chosen?

**Response:** Although the location of the reference point was indicated in our original manuscript as a black star in figure 3, we acknowledge its visibility should be improved and we have modified the figure. The reference point was initially set in the city of Massa because GPS measurements from *Bennett et al. (2012)* show that the surface velocities there are  $< 1\text{mm/yr}$ , therefore, Massa can be considered stable. Assuming Massa as reference point, the retrieved LOS deformation maps revealed the extent of the deformation pattern around the Pieve Fosciana. We then selected a reference point outside the deformation pattern but close to Pieve Fosciana town (white star in Supp. Fig. 3). The reason of this change (that can be done in post processing and does not affect the result accuracy) is due to the fact that the new reference point is closer to our deformation signal than Massa, allowing us to reduce the impact of the atmospheric artefacts in the LOS displacement time series. The tropospheric artefacts are spatially correlated and thus can be considered almost identical in areas close to the reference point. Therefore, by using a reference point close to the deformation signal, the impact of tropospheric disturbances can be minimized. This procedure in summary implies that the quality of the final measurements is improved in the area under study.

**Comment:** SBAS deformation pattern suggests that the subsidence area is much wider than the actual depression revealed by contour lines. SBAS coherence threshold 0.8 is much too high and a map with coherence level at 0.4-0.5 should be drawn to try to display the whole deformation pattern. Of course, there will be much more noise but this is the conditions to get the maximum from the images.

**Response:** We chose a coherence threshold of 0.8 in order to guarantee that only reliable pixels are analysed and interpreted here. The 0.8 value is referred to the threshold used for the phase unwrapping step by the Extended Minimum Cost Flow (EMCF) algorithm. By setting high values of this parameter the pixels in input to the EMCF algorithm are affected by less noise thus increasing the quality of the phase unwrapping step itself. This approach has shown to be also effective in areas affected by low coherence values (*Cignetti et al. 2016*). In any case, according to the Reviewer's request, we reprocessed the data using a coherence threshold of 0.4. The new results are displayed in Supplementary Fig. 3 and show that

only a few more pixels are gained north of the sinkhole as compared to our original results. We conclude that by decreasing the coherence threshold we cannot retrieve the whole deformation pattern. This is likely due to the fact the area is highly vegetated.

**Comment:** SBAS points selected with coherence at 0.8 level indicated important ground movements that should have created series of fissures and fractures in the buildings of the nearby village. The collection of those pieces of evidence is necessary to validate the SBAS observations. Furthermore, those evidences should be linked to the structural context of the depression.

**Response:** There have been no reports of fractures or fissures in the buildings of the village, this is likely because the subsidence pattern is relatively broad compared to the size of a building thus there is no significant strain applied to the buildings. Structural damages are the consequence of high strain rates applied to individual buildings (*Arangio et al., 2013*). The only presence of fractures occurred in an abandoned building in the immediate vicinity of the lake. However, InSAR is not coherent in this area and a direct comparison between the deformation field and the building damage cannot be derived.

## # Reviewer 2

**General Comments:** The authors present an interesting piece of work with interpretations on the activity of one sinkhole in a seismically active zone. Essentially, the work proposes the following conclusions/interpretations: (1) The dynamics of the analysed sinkhole, characterised by progressive subsidence, punctuated by events of more rapid displacement and ground fissuring (1996, 2016), are attributed to creeping faults in the area that induce fracturing, permeability increase and enhanced dissolution. (2) Based on DInSAR data, ground deformation affects a large area around the sink-hole lake with horizontal displacement rates as high as the vertical ones. However, I consider that such conclusions/interpretations are not properly justified, and authors should consider and discuss other alternative interpretations. Concerning point (1), authors should also consider other potential controlling factors such as precipitation and groundwater level changes. Moreover, the available data does not seem to be sufficient to rule out the role of major morphogenetic earthquakes on sinkhole triggering. Authors should review the existing literature that document the formation of coseismic sinkholes in Italy. Regarding point (2), authors should consider the option that ground displacement with significant horizontal component on the NW margin of the sinkhole could be related to a landslide, favoured by debuttressing-undermining at the foot of the slope due to sinkhole subsidence.

**Response:** We are glad that the reviewer finds our results interesting. We agree that seismic creep is one interpretation but other possible source mechanisms should be addressed. We included a geomorphologic map of the Pieve Fosciana area showing that no landslide has been identified in the actively deforming area. Furthermore, the low topographic slope rules out the presence of an active landslide. On the other hand, a recent geochemical study (*Gherardi and Pierrotti, 2018*) shows that waters at Prà di Lama raise from a deep aquifer (~2000 m) along a fractures system. This is in agreement with the presence of a fault and a deep-sited caprock collapse sinkhole (*Gutierrez et al., 2008, 2014*). The horizontal eastward motion derived by InSAR is in agreement with contraction toward the centre of the sinkhole as a result of subsidence. We added this discussion to the paper.

Precipitations can influence the groundwater level and thus ground motions but these patterns have a seasonal trend rather than continuous subsidence over a timespan of several years, as shown by our InSAR analysis. A long-term subsidence could potentially be caused by over-exploitation of an aquifer but no water is pumped from the aquifers in the deforming area. We added this explanation to the manuscript at lines 260-269. Furthermore, the broad subsidence pattern observed at Pieve Fosciana (Fig. 4 and 5) indicates a deep source, likely the 2 km depth carbonatic-evaporite formation. The hypothesis of seismic creep along an active fault remains our favourite interpretation because this mechanism can explain the

variety of observations, ranging from surface subsidence as seen by InSAR, lake level fluctuations documented in the historical record, mapped faults from structural geology and upward fluid migration from geochemistry.

Although the relationship between active faults, creep and surface features, like sinkholes, is a relatively new research topic, it is well established that faults creep both seismically and aseismically (e.g. *Linde et al. 1996; Wei et al. 2013*). In particular, seismic creep has been reported along different active faults (i.e. *Linde et al. 1996, Nadeau et al., 1995; Rau et al., 2007; Chen et al., 2008; Harris, 2017*). Relationships between creeping faults and fluid migration causing enhanced permeability are also widely reported in literature (i.e. *Wei et al., 2009; Scholz, 1998; Yarushina et al., 2017; Sibson, 1996; Micklethwaite et al., 2010*). These observations justify the hypothesis of seismic creep at Prà di Lama because of the presence of an active faults, evidences of deep fluid migration and a mapped sinkhole. We added this explanation to the manuscript together with an expanded section detailing the above-mentioned examples of seismic creep, see changes at lines 280-283.

To strengthen our seismicity analysis and clarify whether a connection between major tectonic earthquakes and sinkhole unrest exists, we analysed both the historical and instrumented seismic catalogues (INGV Catalogo Parametrico dei Terremoti Italiani, CPTI15). We now include a new figure (Fig.8) showing the occurrence of major earthquakes, with magnitude > 4.0 up to 20 km distant from Pieve Fosciana and the recorded events of unrest at the sinkhole. The figure shows that there is no clear connection between occurrence of large distant earthquakes and events of sinkhole unrest, therefore the mechanisms responsible for the Prà di Lama sinkhole formation should be attributed to local processes.

**Comment 2.2:** I believe the sinkhole definition used (lines 29-30) is inadequate since not all the sinkholes form due to cavity collapse. There are other genetic processes. The authors should clearly indicate the type of sinkhole they are investigating, explaining the subsidence mechanisms in relationship with the local stratigraphy. I consider that revising this paper: Parise, M., Closson, D., Gutiérrez, F. et al. *Environ Earth Sci* (2015) 74: 7823. <https://doi.org/10.1007/s12665-015-4647-5>; could help. The cover is underlain by flysch. Do you have deep-seated caprock collapse sinkholes?

**Response:** We modified the sentence “Sinkholes are quasi-circular depressions in the ground surface that form due to the breakdown of subterranean cavities” to “Sinkholes are closed depressions with internal drainage typically associated with karst environments”, following the definitions by *Ford and Williams (2007)* and *Gutiérrez et al. (2008, 2014)*. We then added a brief description of the main genetic processes, as suggested by the reviewer, and clarified that we study a sinkhole classified as deep-sited caprock collapse sinkhole, according to *Gutiérrez et al. (2008, 2014)*. We explained the subsidence mechanisms in relationship with the local stratigraphy by clarifying that collapse of deep cavities caused by fluid circulation occurs in carbonatic-evaporitic formations located at 1.3-2 km depth and covered by a thick non-carbonatic sequence. See changes at lines 29-49.

**Comment 2.3:** The authors conclude that “a source mechanism for the sinkhole formation and growth is seismic creep in the active fault zone underneath the sinkhole”. Although this hypothesis looks innovative, it is not well supported by the presented data. The casual relationship between creep tectonic deformation and sinkhole activity remains as an unproved hypothesis. I encourage the authors to add sub-subface geophysical and structural data to test their hypothesis.

**Response:** We agree that the explanation of a tectonic-induced sinkhole is new and we provided a new structural geology map (Fig 2a) as well as a geology cross-section (Fig. 2c) showing that faults geometries are consistent with a structural control on the sinkhole. We also added a discussion section including examples of active faults characterized by seismic creep analogous to our case. In particular we presented

the examples of Taiwan (*Rau et al., 2007; Chen et al., 2008; Harris, 2017*) and Parkfield (California) (*Nadeau et al., 1995; Harris, 2017*).

#### List of relevant changes

- **Line 3.** Prof. Giacomo D'amato Avanzi (Dipartimento di Scienze della Terra – Università di Pisa) has been added as co-author of the paper for his contribution of geomorphological information in Pieve di Fosciana.
- **Lines 29-32.** The sentence "Sinkholes are quasi-circular depressions in the ground surface that form due to the breakdown of subterranean cavities" has been modified to "Sinkholes are closed depressions with internal drainage typically associated with karst environments", following the definition by *Ford and Williams (2007)* and *Gutierrez et al. (2008, 2014)*
- **Lines 33-49.** A better description of the several types of sinkholes has been provided following the classification of *Gutierrez et al. (2008, 2014)* and by referring to *Del Prete et al. (2010)* *Parise et al., (2010)*, as suggested by the editor
- **Lines 50-54.** A more complete review of Italian seismically-induced sinkholes has been provided by referring to *Parise and Vennari (2013)*, *Parise et al. (2010)*, *Kawashima et al. (2010)*, *Santo et al. (2007)*, as suggested by the editor.
- **Lines 88-90.** The stratigraphic sequence of Prà di Lama lake has been completed by describing the deeper formations.
- **Lines 91-95.** We added a description of the geomorphological features characterizing the Prà di Lama lake.
- **Lines 100-109.** The geochemical analyses of the Prà di Lama springs and the related conclusions provided by *Gherardi and Pierotti (2018)* have been added to our manuscript to better constrain our hypotheses.
- **Lines 161-166.** We have added a section describing the role of the coherence threshold in the InSAR P-SBAS processing.
- **Lines 174-181.** We have added a section to describe the selection of the reference point and its effect on the final results
- **Lines 189-203.** We have added a section showing the results of the processing test using a coherence threshold of 0.4, as suggested by the referees
- **Lines 242-249.** In the seismicity chapter, we have added a section containing the results of the analysis of the Historical Catalogue (CPTI15) and we have shown the lack of correspondence between strong historical earthquakes and events of unrest at Prà di Lama
- **Lines 258-267.** We considered other geological processes that could explain the observed deformation at Prà di Lama, as suggested by the referees

- **Lines 283-286.** We included the geochemical analysis of spring waters (*Gherardi and Pierotti, 2018*) in our discussion.
- **Lines 286-288.** We classified the Prà di Lama sinkhole as a deep-sited caprock collapse sinkhole using the classification of *Gutierrez et al. (2008, 2014)*, as suggested by the editor
- **Figure 1** has been modified to show that the Prà di Lama sinkhole is an isolated feature in the region being the only mapped sinkhole in the entire Garfagnana graben. In Particolare, a red dot has been added to indicate the Camaiore sinkhole and a yellow star has been used to indicate the Prà di Lama sinkhole.
- **Figure 2** This is a new figure. It consists of a geological, geomorphological and structural map (Fig. 2a) accompanied by a shallow stratigraphic log from *Chetoni (1995)* (Fig 2b) and a geological cross-section (Fig 3).
- **Figure 3** has been modified to better show the fracture pattern formed during the unrest event of 1996.
- **Figure 8** has been added to show the comparison between the historical seismic catalogue and the events of unrest at Prà di Lama.
- **Supplementary material** has been included. Supplementary material 1 and 2 contain pictures of the two recent events of unrest at Prà di lama (1996, 2016). Supplementary material 3 show the InSAR processing results using a coherence threshold of 0.4.

1 GROWTH OF A SINKHOLE IN A SEISMIC ZONE OF THE NORTHERN APENNINES (ITALY)

2 Alessandro La Rosa<sup>1,2</sup>, Carolina Pagli<sup>2</sup>, Giancarlo Molli<sup>2</sup>, Francesco Casu<sup>3</sup>, Claudio De Luca<sup>3</sup>,  
3 Amerino Pieroni<sup>4</sup> and Giacomo D'amato Avanzi<sup>2</sup>

4

5 <sup>1</sup> Dipartimento di Scienze della Terra, Università degli Studi di Firenze, Via G. La Pira, 4, 50121 Firenze, Italy

6 <sup>2</sup> Dipartimento di Scienze della Terra, Università di Pisa, Via S. Maria, 53, 56126 Pisa, Italy

7 <sup>3</sup> CNR, Consiglio Nazionale delle Ricerche, Istituto per il Rilevamento Elettromagnetico dell'Ambiente (IREA-  
8 CNR), Via Diocleziano, 328, 80124 Napoli, Italy

9 <sup>4</sup> Pro.Geo. s.r.l. Via Valmaira, 14, 55032, Castelnuovo di Garfagnana, Italy

10

11 **Keywords:** Sinkhole, InSAR, Seismicity

12 **Abstract**

13 Sinkhole collapse is a major hazard causing substantial social and economic losses. However,  
14 the surface deformations and sinkhole evolution are rarely recorded, as these sites are known  
15 mainly after a collapse, making the assessment of sinkholes-related hazard challenging.

16 Furthermore, more than 40% of the sinkholes of Italy are in seismically hazardous zones; it  
17 remains unclear whether seismicity may trigger sinkhole collapse. Here we use a multidisciplinary

18 dataset of InSAR, surface mapping and historical records of sinkhole activity to show that the Prà  
19 di Lama lake is a long-lived sinkhole that was formed over a century ago in active fault zone and

20 grew through several events of unrest characterized by episodic subsidence and lake-level  
21 changes. Moreover, InSAR shows that continuous aseismic subsidence at rates of up to 7.1 mm yr<sup>-1</sup>

22 <sup>1</sup> occurred during 2003-2008, between events of unrest. Earthquakes on the major faults near the  
23 sinkhole are not a trigger to sinkhole activity but small-magnitude earthquakes at 4-12 km depth

24 occurred during sinkhole unrest in 1996 and 2016. We interpret our observations as evidence of  
25 seismic creep in an active fault zone at depth causing fracturing and ultimately leading to the

26 formation and growth of the Prà di Lama sinkhole.

27

## 28 1. Introduction

29 ~~Sinkholes are quasi circular depressions in the ground surface that form due to the~~  
30 ~~breakdown of subterranean cavities (Neuendorf et al., 2005)~~ Sinkholes are closed depressions with  
31 internal drainage typically associated with karst environments, where the exposed soluble rocks  
32 are dissolved by circulating ground water (dissolution sinkholes) but other types of sinkholes also  
33 exist. Subsidence sinkholes, for example, can form for both internal erosion and dissolution of  
34 covered layers leading to downward gravitational deformations such as collapse, sagging or  
35 suffosion (Ford and Williams, 2007; Gutiérrez et al., 2008; Gutiérrez et al., 2014). Deep sinkholes  
36 have been often observed along seismically active faults indicating a causal link between sinkhole  
37 formation and active tectonics (Faccenna et al., 1993; Closson et al., 2005; Florea, 2005; Harrison  
38 et al., 2002; Del Prete et al., 2010; Parise et al., 2010; Wadas et al., 2017). In some cases, tThe  
39 processes responsible for the formation of these sinkholes have been attributed to fracturing and  
40 increased permeability in the fault damage zone promoting fluid circulation and weathering of  
41 soluble rocks at depth. Additionally, when carbonate bedrocks lie below thick non-carbonate  
42 formations, stress changes caused by faulting may cause decompression of confined aquifers  
43 favouring upward migration of deep ~~acid~~ fluids hence promoting erosion and collapses (e.g.  
44 Harrison et al., 2002; Wadas et al., 2017); ~~a process known as Deep Piping (Caramanna et al.,~~  
45 ~~2008)~~ Seismically-induced stress changes could also trigger collapse of unstable cavities. -as in the  
46 case of the two Sinkhole formation can also be triggered by faulting and two sinkholes that formed  
47 near En Gedi (Dead Sea) following the Mw 5.2 earthquake on the Dead Sea Transform Fault in 2004  
48 (Salamon, 2004). Sinkhole subsidence and collapses are a major hazard and cause substantial  
49 economic and human losses globally (Frumkin and Raz, 2001; Wadas, 2017; Closson, 2005).

50 In Italy, a total of 750 sinkholes have been identified and the 40% of them are along active  
51 faults (Caramanna et al., 2008) but this number could be underestimated due to the high

52 frequency of sinkholes both related to karst and anthropogenic origin (Parise and Vennari, 2013).  
53 Seismicity induced sinkhole deformation have been often observed in Italy (e.g. Parise et al., 2010;  
54 Kawashima et al., 2010; Santo et al., 2007).

55 The sinkhole of Prà di Lama, near the Pieve Fosciana town (Lucca, Italy), is a quasi-circular  
56 depression filled by a lake. ~~(Caramanna et al., 2008)~~. Prà di Lama is located in the seismically  
57 active Apennine range of Northern Tuscany, at the intersection between two active faults (Fig. 1).  
58 Hot springs are also present at Pieve Fosciana suggesting that fluid migration along the faults  
59 planes occurs. Sudden lake-level changes of up to several meters, ground subsidence, surface  
60 fracturing and seismicity have occurred repeatedly since at least 991 A.D. (Nisio, 2008). The most  
61 recent deformation events occurred in March 1996 and between May 2016 and October 2017.  
62 However, the processes that control the growth of the Prà di Lama sinkhole remain unclear.  
63 Furthermore, whether seismicity along the active faults around Prà di Lama may trigger sinkhole  
64 subsidence or collapse is debated.

65 In this paper we combine recent InSAR observations, seismicity, and surface mapping, as  
66 well as historical records of lake-level changes and ground subsidence at the Prà di Lama from  
67 1828 to understand the mechanisms of sinkhole growth in an active fault system.

## 68 **2. Geological setting**

69 The area of the Prà di Lama sinkhole is located within the Garfagnana basin (Fig.1), an  
70 extensional graben in the western Northern Apennines, a NW-SE trending fold-and-thrust belt  
71 formed by the stack of different tectonic units caused by the convergence of the Corsica-European  
72 and Adria plates. The current tectonic regime of the Apennines is characterized by shortening in  
73 the eastern sector of the Apennine range and extension in the westernmost side of the range  
74 (Elter et al., 1975; Patacca and Scandone, 1989; Bennett et al., 2012). The contemporaneous  
75 eastward migration of shortening and upper plate extension are believed to be caused by the roll-

76 back subduction during the counter-clockwise rotation of the Adria plate (*Doglioni, 1991; Meletti*  
77 *et al., 2000; Serpelloni et al., 2005; Faccenna et al., 2014; Le Breton et al., 2017*). Extension started  
78 4-5 Ma ago leading to the formation of several NW-SE-oriented grabens, bounded by NE-dipping  
79 and SW-dipping normal faults that are dissected by several NE-trending, right-lateral strike-slip  
80 faults (Fig. 1). The inner northern Apennines are a seismically active area, where several  
81 earthquakes with  $M_w > 5$  occurred, including the largest instrumentally recorded earthquake,  $M_w$   
82 6.5, in 1920 (*Tertulliani and Maramai, 1998; Rovida et al., 2016; Bonini et al., 2016*) and the most  
83 recent  $M_w$  5.1 earthquake in 2013 (*Pezzo et al., 2014; Stramondo et al., 2014; Molli et al., 2016*).

84 The uppermost stratigraphy at Prà di Lama consists of an 8m-thick layer of alluvial and  
85 palustrine gravels and sandy deposits containing pity levels, covering an ~85m-thick sandy-to-silty  
86 fluvio-lacustrine deposits with low permeability (from Villafranchian to present age) (*Chetoni,*  
87 *1995*) (Fig.2a and b). These deposits cover a ~1000m-thick turbiditic sequence (Macigno Fm).  
88 Below it, a sequence of carbonate rocks pertaining to the Tuscan Nappe Unit is present reaching  
89 down to a depth of ~2000 m, where anhydrites (Burano fm.) and calcareous-dolomitic breccias  
90 (Calcare Cavernoso Fm.) overlie the Tuscan Metamorphic Units (Fig. 2c).

91 The Prà di Lama lake lies at the centre of a depression (Fig. 2 and 5). The low slopes  
92 characterizing the topography of the area results in the absence of active gravitational ground  
93 motions (Fig 2). Furthermore, the Prà di Lama sinkhole is an isolated feature in the region being  
94 the only mapped sinkhole in the entire Garfagnana graben (Caramanna et al., 2008); the closest  
95 sinkhole is in Camaiore (Lucca) near the Tuscany coast (Fig.1).

96 The Prà di Lama sinkhole is located at the intersection between two seismically active faults:  
97 the Corfino normal fault (*Di Naccio et al., 2013; Itacha working group, 2003; ISIDe working group,*  
98 *2016*) and the right-lateral strike-slip fault M.Perpoli-T.Scoltenna that recently generated the  $M_w$   
99 4.8 earthquake in January 2013 (Fig.1) (*Vannoli, 2013; Pinelli, 2013; Molli et al., 2017*). Hot water

100 springs are also present at Prà di Lama (*Bencini et al., 1977; Gherardi and Pierotti, 2018*) ~~and some~~  
101 ~~of them have a water temperature of ~40 °C (*Bencini et al., 1977*).~~ Geochemical analyses of the Prà  
102 di Lama spring waters by *Gherardi and Pierotti (2018)*, expanding on previous research (*Baldacci et*  
103 *al., 2007*), suggest that both shallow and deep aquifers are present below Prà di Lama (Fig. 2b).  
104 Shallow aquifers have low salinity and low temperature while waters feeding the thermal springs  
105 have high temperature (~57 °C) and high salinity (5.9g/kgw), suggesting the presence of a deep  
106 aquifer at ~2000 m into the anhydrite and the calcareous-dolomitic breccia. The high salinity of  
107 the deep groundwaters is associated with dissolution of the deep evaporitic formations.  
108 Furthermore, un-mixing of deep and shallow waters is interpreted by *Gherardi and Pierotti (2018)*  
109 as an evidence of their rapid upwelling likely occurring along the existing faults.

110 ~~Prà di Lama was classified as a Deep Piping Sinkhole (DPS) as it is a circular depression that~~  
111 ~~formed on thick impermeable sediments in a fracture zone, likely due to erosion of soluble rocks~~  
112 ~~at depth (*Caramanna et al., 2008*). Hot springs are also a common feature of DPSs due to the~~  
113 ~~presence of pressurized aquifers together with a system of fractures favouring fluid circulation.~~

### 114 **3. Data**

115 Century-scale historical records of sinkhole activity are available at Prà di Lama and allow us  
116 to determine the timescale of sinkhole evolution as well as to characterize the different events of  
117 unrest, in particular the two most recent events in 1996 and 2016. InSAR time-series analysis is  
118 also carried out to measure ground deformations in the Prà di Lama sinkhole in the time period  
119 between events of unrest. Finally, the local catalogue of seismicity (ISIDE catalogue, INGV) is used  
120 to inform us on the timing and types of brittle failures in the area of the sinkhole.

#### 121 **3.1 Historical Record**

122 The first historical record of the Prà di Lama sinkhole dates back to the 991 A.D., when the  
123 area was described as a seasonal shallow pool fed by springs. Since then, the depression grew and

124 several events of unrest consisting of fracturing and fluctuations of the lake level were reported  
125 (*Raffaelli, 1869; De Stefani, 1879, Giovannetti, 1975*) (Table 1). In particular, eight events of unrest  
126 were reported, giving an average of 1 event of unrest every 26 years. We conducted direct  
127 observation of surface deformation around the lake for the two most recent events in 1996 and  
128 2016.

129 In 1996, the lake level experienced a fall of up to 4 m (Fig. [32](#) and [Fig. S1](#)) and at the same  
130 time the springs outside the lake suddenly increase the water outflow. Clay and mud were also  
131 ejected by the springs outside the lake while fractures and slumps occurred within the lake due to  
132 the water drop (Fig. [32](#) and [Fig. S1](#)). The unrest lasted approximately 2 months, from March to  
133 April 1996. During the final stages, the water level in the lake rose rapidly recovering its initial level  
134 and contemporaneously the springs water flow reduced.

135 In June 2016, an event of unrest consisting of ground subsidence on the western and southern  
136 sides of the Prà di Lama lake started and lasted approximately 9 months, until February 2017.  
137 During this period fractures formed and progressively grew, increasing their throw to up to 70 cm  
138 and affecting a large area on the western side of the lake (Fig. [32](#) and [Fig. S2](#)). Subsidence around  
139 the lake resulted in an increase of the lake surface in particular on the western side and formation  
140 of tensile fractures (Fig. [32](#) and [Fig. S2](#)). Unlike the 1996 events of unrest, no lake level changes or  
141 increase of water flow from the springs around the lake were observed.

### 142 **3.2 InSAR**

143 InSAR is ideally suited to monitor localized ground deformation such as caused by sinkholes  
144 as it can observe rapidly evolving deformation of the ground at high spatial resolution (*Baer et al.,*  
145 *2002; Castañeda et al., 2009; Atzori et al., 2015; Abelson et al., 2017*). Furthermore, the availability  
146 of relatively long datasets of SAR images in the Apennine allows us to study the behaviour of the  
147 Prà di Lama sinkhole using multi-temporal techniques. We processed a total of 200 interferograms

148 using SAR images acquired by the ENVISAT satellite between 2003 to 2010 from two distinct tracks  
149 in Ascending or Descending viewing geometry (tracks 215 and 437). We used the Small Baseline  
150 Subset (SBAS) multi-interferogram method originally developed by *Berardino et al. (2002)* and  
151 recently implemented for parallel computing processing (P-SBAS) by *Casu et al. (2014)* to obtain  
152 incremental and cumulative time-series of InSAR Line-of-Sight (LOS) displacements as well as maps  
153 of average LOS velocity. In particular, the InSAR processing has been carried out via the ESA  
154 platform P-SBAS open-access on-line tool named G-POD (Grid Processing On Demand) that allows  
155 generating ground displacement time series from a set of SAR data (*De Luca et al., 2015*).

156 The P-SBAS G-POD tool allows the user to set some key parameters to tune the InSAR  
157 processing. In this work, we set a maximum perpendicular baseline (spatial baseline) of 400 m and  
158 maximum temporal baseline of 1500 days. The geocoded pixel dimension was set to ~80 m by 80  
159 m (corresponding to averaging together 20 pixels in range and 4 pixels in azimuth).

160 We initially set a coherence threshold to 0.8 (0 to 1 for low to high coherence) in order to  
161 select only highly coherent pixels in our interferograms. The 0.8 coherence threshold is used to  
162 select the pixels for the phase unwrapping step that is carried out by the Extended Minimum Cost  
163 Flow (EMCF) algorithm (*Pepe and Lanari, 2006*). By setting high values of this parameter the pixels  
164 in input to the EMCF algorithm are affected by less noise as compared to selecting low values, thus  
165 increasing the quality of the phase unwrapping step itself and reducing the noise in our final  
166 velocity maps and time-series (*De Luca et al., 2015; Cignetti et al., 2016*).

167 We also inspected the series of interferograms and excluded individual interferograms with  
168 low coherence. We identified and discarded 29 noisy interferograms in track 215A and other 11  
169 interferograms in track 437D. Finally, we applied an Atmospheric Phase Screen (APS) filtering to  
170 mitigate further atmospheric disturbances (*Hassen, 2001*). Accordingly, we used a triangular  
171 temporal filter with a width of 400 days to minimize temporal variations shorter than about a year

172 as we focus on steady deformations rather than seasonal changes. Shorter time interval of 300  
173 days was also tested but provided more noisy time-series.

174 The average velocity map and the incremental time-series of deformation obtained with the  
175 P-SBAS method have to be referred to a stable Reference Point. For our analysis, the reference  
176 point was initially set in the city of Massa because GPS measurements from *Bennett et al. (2012)*  
177 show that the surface velocities there are < 1mm/yr, therefore, Massa can be considered stable.  
178 Assuming Massa as reference point, the average velocity map revealed the deformation pattern  
179 around the Prà di Lama lake. We then moved the reference point outside the sinkhole  
180 deformation pattern but close to Pieve Fosciana town (Fig. S3a). Selecting a reference point close  
181 to our study area rather than in Massa allowed us to better minimize the spatially correlated  
182 atmospheric artefacts.

183 As a ~~final~~<sup>urther</sup> post processing step we also calculated the vertical and east-west components  
184 of the velocity field in the area covered by both the ascending and descending tracks and assuming  
185 no north-south displacement. Given that the study area is imaged by the ENVISAT satellite from  
186 two symmetrical geometries with similar incidence angles (few degrees of difference), the vertical  
187 and east-west components of the velocity field can simply be obtained solving the following  
188 system of equations (*Manzo et al., 2006*):

$$189 \begin{cases} v_H = \frac{\cos \vartheta}{\sin(2\vartheta)} (v_{DESC} - v_{ASC}) = \frac{v_{DESC} - v_{ASC}}{2 \sin \vartheta} \\ v_V = \frac{\sin \vartheta}{\sin(2\vartheta)} (v_{DESC} + v_{ASC}) = \frac{v_{DESC} + v_{ASC}}{2 \cos \vartheta} \end{cases}$$

190 where  $v_H$  and  $v_V$  are the horizontal and vertical component of the velocity field,  $v_{DESC}$  and  $v_{ASC}$   
191 are the average LOS velocities in the Descending and Ascending tracks, respectively;  $\vartheta$  is the  
192 incidence angle.

193 The InSAR P-SBAS analysis shows that significant surface deformation occurs at Pieve  
194 Fosciana between 2003 and 2010. The observed deformation pattern consists of range increase

195 mainly on the western flank of the Prà di Lama lake. The range increase is observed in both  
196 ascending and descending velocity maps (Fig. [43a, b](#)), with average LOS velocities of up to  $-7.1 \text{ mm}$   
197  $\text{yr}^{-1}$  decaying to  $-1 \text{ mm yr}^{-1}$  over a distance of 400 m away from the lake. Elsewhere around the lake  
198 coherence is not kept due to ground vegetation cover but few coherent pixels on eastern flank of  
199 the lake suggest that the deformation pattern may be circular, with a radius of  $\sim 600 \text{ m}$  (Fig. [4 and](#)  
200 [5](#)). In order to increase the number of analysed pixels we tested decreasing our coherence  
201 threshold from 0.8 to 0.4. The results are displayed in Fig. S3b and show that only a few more  
202 pixels are gained north of the sinkhole as compared to choosing a threshold of 0.8 (Fig. 4). We  
203 conclude that decreasing the coherence threshold does not allow to retrieve the entire  
204 deformation pattern, likely due to the fact the area is vegetated.

205 The maps of vertical and East-West velocities show vertical rates of  $-4.6 \text{ mm yr}^{-1}$  and horizontal  
206 eastward velocities of  $5.4 \text{ mm yr}^{-1}$  (Fig. [43c, d](#)) consistent with subsidence and contraction centred  
207 at the lake. Furthermore, figure [54](#) shows that the current deformation pattern follows the  
208 topography, suggesting that subsidence at Prà di Lama is a long-term feature. The time-series of  
209 cumulative LOS displacements show that subsidence occurred at an approximately constant rate  
210 between the 2003 and the 2008 but it slowed down in 2008 (Fig. [43e, f](#)), indicating that  
211 subsidence at Prà di Lama occurs also between events of unrest. Furthermore, our time-series of  
212 vertical and east-west cumulative displacements also confirm that the fastest subsidence and  
213 contemporaneous eastward motion occurred until 2008 (Fig. [43 g, h](#)). In order to better  
214 understand the mechanisms responsible for the sinkhole growth and the different types of  
215 episodic unrest we also analysed the seismicity.

### 216 **3.3 Seismicity**

217 We analysed the seismicity at the Prà di Lama lake using the catalogue ISIDe (Italian  
218 Seismological Instrumental and Parametric Data-Base) spanning the time period from 1986 to

219 2016. We calculated the cumulative seismic moment release using the relation between seismic  
220 moment and magnitudes given by *Kanamori (1977)*. First, we analysed the seismic moment  
221 release and the magnitude content of the earthquakes in the area encompassing the sinkhole and  
222 the faults intersection (10 km radius, Fig. 1) to understand whether unrest at Prà di Lama is  
223 triggered by earthquakes along the active faults (Fig. 65). Fig. 46a shows that although several  
224 seismic swarms occurred in the area, no clear temporal correlation between the swarms and the  
225 events of unrest at Prà di Lama is observed, suggesting that the majority of seismic strain released  
226 on faults around the Prà di Lama lake does not affect the activity of the sinkhole. We removed  
227 from the plot in Fig. 64a the large magnitude earthquake,  $M_w$  4.8, on the 25<sup>th</sup> of January 25, 2013  
228 in order to better visualize the pattern of seismic moment release in time. In any case, no activity  
229 at Prà di Lama was reported in January 2013.

230 We also analysed the local seismicity around the Prà di lama lake, within a circular area of 3  
231 km radius around the lake (Fig. 1), to better understand the deformation processes occurring at  
232 the sinkhole (Fig. 6) and we found that swarms of small-magnitude earthquakes ( $M_L \leq 2$ ) occurred  
233 during both events of unrest at Prà di Lama in 1996 and 2016 (Fig. 76a, b, c), while a few  
234 earthquakes with magnitudes  $> 2$  occurred irrespective of the events of unrest. This indicates that  
235 seismicity during sinkhole activity is characterized by seismic energy released preferentially  
236 towards the small end of magnitudes spectrum. This pattern is specific of the sinkhole area as in  
237 the broader region (Fig. 65b, c) the majority of earthquakes magnitudes are in the range between  
238  $M_L > 2$  and  $M_L < 3$  and few  $M_L > 3$  also occurred. We also analysed the hypocentres of the  
239 earthquakes around the Prà di lama lake (3 km radius) and find that these range between 4.5 and  
240 11.5 km depth, indicating that deformation processes in the fault zone control the sinkhole  
241 activity. On the other hand, no earthquakes were recorded at Prà di Lama during the period of

242 subsidence identified by InSAR between 2003 and 2010, indicating that subsidence between  
243 events of unrest continues largely aseismically.

244 To strengthen our seismicity analysis and clarify whether a connection between major  
245 tectonic earthquakes and sinkhole unrest exists, we also analysed the historical parametric seismic  
246 catalogues (Rovida et al., (2016), INGV Catalogo Parametrico dei Terremoti Italiani, CPTI15). Figure  
247 8 shows the occurrence of major earthquakes, with magnitude > 4.0 up to 20 km distant from  
248 Pieve Fosciana and the events of sinkhole unrest at Pra di lama. No clear connection between  
249 occurrence of large distant earthquakes and events of sinkhole unrest is observed, suggesting that  
250 the mechanisms responsible for activation of the Prà di Lama sinkhole should be attributed to  
251 local processes.

#### 252 4. Discussion and conclusions

253 A multi-disciplinary dataset of InSAR measurements, field observations and seismicity reveal  
254 that diverse deformation events occur at the Prà di Lama sinkhole. Two main events of sinkhole  
255 unrest occurred at Prà di Lama in 1996 and 2016 but the processes had different features. In 1996  
256 the lake-level dropped together with increased water outflow from the springs, while in 2016  
257 ground subsidence led to the expansion of the lake surface and fracturing. In 2016, fractures form  
258 in the South-Western shore of the lake. The main active strike-slip fault is also oriented SW,  
259 suggesting a possible tectonic control on the deformation.

260 We also considered processes not related to the sinkhole activity that could explain the  
261 observed deformation at Prà di Lama. Active landslides can cause both vertical and horizontal  
262 surface motions (e.g. Nishiquchi et al., 2017). However, no landslides are identified in the  
263 deforming area around the sinkhole (Fig.3). Furthermore, the low topographic slopes rule out the  
264 presence of active landslides in the area. Concentric deformation patterns are observed above

265 shallow aquifers (e.g. Amelung et al., 1999). However, deformation caused by aquifers have a  
266 seasonal pattern rather than continuous subsidence over the timespan of several years, as in Pra  
267 di Lama. A long-term subsidence could only be caused by over-exploitation of an aquifer but no  
268 water is pumped from the aquifers in the deforming area around Pra di Lama. We conclude that  
269 the observed InSAR deformation is caused by the sinkhole.

270 ~~Furthermore,~~ InSAR analysis shows that continuous but aseismic subsidence of the sinkhole  
271 occurred between the two events of unrest, during the period 2003-2010. Instead swarms of  
272 small-magnitude earthquakes coeval to the unrest events of 1996 and 2016 were recorded at  
273 depth between 4.5 and 11.5 km, indicating that a link between low magnitude seismicity and  
274 sinkhole activity exists. We suggest that seismic creep in the fault zone underneath Prà di Lama  
275 occurs, causing the diverse deformation events.

276 Seismic creep at depth could have induced pressure changes in the aquifer above the fault  
277 zone (1996 events) as well as causing subsidence by increased fracturing (2016 events). The  
278 seismicity pattern revealed by our analysis suggests that the Mt.Perpoli-T.Scoltenna strike-slip  
279 fault system underneath Prà di Lama is locally creeping, producing seismic sequences of low  
280 magnitude earthquakes. Similar seismicity patterns were observed along different active faults  
281 (i.e. Linde et al. 1996, Nadeau et al., 1995; Rau et al., 2007; Chen et al., 2008; Harris, 2017). In  
282 2006, along the Superstition Hills fault (San Andreas fault system, California) ~~where~~ seismic creep  
283 has been ~~is~~ favoured by high water pressure (Wei et al., 2009; Scholz, 1998; Harris, 2017). We  
284 suggest that along the fault zone below Prà di Lama an increase in pressure in the aquifer in 1996  
285 caused fracturing at the bottom of the lake and upward migration of fluids rich in clays, in  
286 agreement with the observations of lake-level drop and mud-rich water ejected by the springs in  
287 1996. Our interpretations is also in agreement with geochemical data indicating that the high  
288 salinity of thermal waters at Prà di Lama have a deep origin, ~2000 m, where fluid circulation

289 dissolves evaporites and carbonates, creating cavities and then reaching the surface by rapid  
290 upwelling along the faults system (Gerardi and Pierotti, 2018). The presence of deep cavities and a  
291 thick non-carbonate sequence suggests that the Prà di Lama sinkhole is a deep-sited caprock  
292 collapse sinkhole according to the sinkhole classification of Gutiérrez et al. (2008, 2014). Sudden  
293 fracturing and periods of compaction of cavities created by enhanced rock dissolution and upward  
294 erosion in the fluid circulation zone could explain both sudden subsidence and fracturing, as in  
295 2016, and periods of continuous but aseismic subsidence as in 2003-2010. Similar processes have  
296 been envisaged for the formation of a sinkhole at the Napoleonville Salt Dome, where a seismicity  
297 study suggests that fracturing enhanced the rock permeability, promoting the rising of fluids and,  
298 as a consequence, erosion and creation of deep cavities prone to collapse (Yarushina et al., 2017;  
299 Sibson, 1996; Micklethwaite et al., 2010, Nayak and Dreger, 2014). Recently, a sequence of seismic  
300 events was identified at Mineral Beach (Dead Sea fault zone) and was interpreted as the result of  
301 cracks formation and faulting above subsurface cavities (Abelson et al., 2017).

302 Precursory subsidence of years to few months has been observed to precede sinkhole  
303 collapse in carbonate or evaporitic bedrocks (e.g. Baer et al., 2002; Nof et al., 2013; Cathleen and  
304 Bloom, 2014; Atzori et al., 2015; Abelson et al., 2017). However, the timing of these processes  
305 strongly depends on the rheological properties of the rocks (Shalev and Lyakhovsky, 2013).  
306 Furthermore, the presence of a thick lithoid sequence in Prà di Lama may delay sinkhole collapse,  
307 also in agreement with the exceptionally long timescale (~200 years) of growth of the Prà di Lama  
308 sinkhole (~~Carammanna et al., 2008~~; Shalev and Lykovsky, 2012; Abelson et al., 2017). However, at  
309 present we are not able to establish if and when a major collapse will occur in Prà di Lama.

310 We identified a wide range of surface deformation patterns associated with the Prà di Lama  
311 sinkhole and we suggest ~~conclude~~ that a source mechanism for the sinkhole formation and growth  
312 is seismic creep in the active fault zone underneath the sinkhole. This mechanism could control

313 the evolution of other active sinkholes ~~DPSs~~ in Italy as well as in other areas worldwide where  
314 sinkhole form in active fault systems (e.g. Dead Sea area). InSAR monitoring has already shown to  
315 be a valid method to detect precursory subsidence occurring before a sinkhole collapse and the  
316 recent SAR missions, such as the European Sentinel-1, will very likely provide a powerful tool to  
317 identify such deformations.

318

## 319 **References**

320

321 Abelson, M., Aksinenko, T., Kurzon, I., Pinsky, V., Baer, G., Nof, R., & Yechieli, Y.: Nanoseismicity forecast  
322 sinkhole collapse in the Dead Sea coast years in advance. <https://doi.org/10.1130/G39579.1> (2017)

323 Amelung, F., Galloway, D.L., Bell, J.W., Zebker, H.A., and Lacznik, R.J.: Sensing the ups and downs of Las  
324 Vegas: InSAR reveals structural control of land subsidence and aquifer-system deformation. *Geology*,  
325 27 (6), 483-486. [https://doi.org/10.1130/0091-7613\(1999\)027<0483:STUADO>2.3.CO;2](https://doi.org/10.1130/0091-7613(1999)027<0483:STUADO>2.3.CO;2) (1999)

326 Atzori, S., Baer, G., Antonioli, A., & Salvi, S.: InSAR-based modelling and analysis of sinkholes along the Dead  
327 Sea coastline. *Geophysical Research Letters*, 42, 8383–8390. <https://doi.org/10.1002/2015GL066053>  
328 (2015)

329 Baldacci, F., Botti, F., Cioni, R., Molli, G., Pierotti, L., Scozzari, A., Vaselli, L.: Geological-structural and  
330 hydrogeochemical studies to identify sismically active structures: case history from the Equi Terme-  
331 Monzone hydrothermal system (Northern Apennine – Italy). *Geitalia, 6th Italian Forum of Earth*  
332 *Sciences. Rimini* (2007).

333 Bencini, A., Duchi, V., Martini, M.: Geochemistry of thermal springs of Tuscany (Italy). *Chemical Geology*, 19,  
334 229-252. (1977)

335 Baer, G., Schattner, U., Wachs D., Sandwell, D., Wdowinski, S., Frydman, S.: The lowest place on Earth is  
336 subsiding – An InSAR (Interferometric Synthetic Aperture Radar) Perspective. *Geological Society of*  
337 *America Bulletin*, 114 (1), 12-23. [https://doi.org/10.1130/00167606\(2002\)114<0012:TLPOEI>2.0.CO;2](https://doi.org/10.1130/00167606(2002)114<0012:TLPOEI>2.0.CO;2)  
338 (2002)

339 Bennet, R.A., Serpelloni, E., Hreinsdottir, S., Brandon, M.T., Buble, G., Basic T., Casale, G., Cavaliere, A.,  
340 Anzidei, M., Marjonovic, Minelli, G., Molli, G., & Montanari, A.: Syn-convergent extension observed  
341 using the RETREAT GPS network, northern Apennines, Italy. *Journal of Geophysical Research*, 117.  
342 <https://doi.org/10.1029/2011JB008744> (2012)

343 Berardino, P., Fornaro, G., Lanari, R., & Sansosti, E.: A new algorithm for surface deformation monitoring  
344 based on Small Baseline Differential SAR interferograms. *IEEE International Geoscience and Remote*  
345 *Sensing Symposium*, 40(11). <https://doi.org/10.1109/TGRS.2002.803792> (2002)

346 Bonini, M., Corti, G., Donne, D. D., Sani, F., Piccardi, L., Vannucci, G., Genco, R., Martelli, L., Ripepe, M.:  
347 Seismic sources and stress transfer interaction among axial normal faults and external thrust fronts in

- 348 the northern Apennines (Italy): a working hypothesis based on the 1916-1920 time-space cluster of  
349 earthquakes. *Tectonophysics*, 680, 67–89. <https://doi.org/10.1016/j.tecto.2016.04.045> (2016)
- 350 Caramanna, G., Ciotoli, G., Nisio, S.: A review of natural sinkhole phenomena in Italian plain areas. *Natural*  
351 *Hazards*, 45, 145–172. <https://doi.org/10.1007/s11069-007-9165-7> (2008)
- 352 Castañeda, C., Gutiérrez, F., Manunta, M., Galve, J. P.: DInSAR measurements of ground deformation by  
353 sinkholes, mining subsidence, and landslides, Ebro River, Spain. *Earth Surf. Process. Landforms*, 34, 11,  
354 1562–1574. <https://doi.org/10.1002/esp.1848> (2009)
- 355 Casu, F., Elefante, S., Imperatore, P., Zinno, I., Manunta, M., De Luca, C., & Lanari, R: SBAS-DInSAR parallel  
356 processing for deformation time-series computation. *IEEE Journal of Selected Topics in Applied Earth*  
357 *Observations and Remote Sensing*, 7(8), 3285–3296. <https://doi.org/10.1109/JSTARS.2014.2322671b>  
358 (2014)
- 359 Cathleen, J., & Blom, R.: Bayou Corne, Louisiana, sinkhole: Precursory deformation measured by radar  
360 interferometry. *Geology*. 42 (2), 111-114. <https://doi.org/10.1130/G34972.1> (2014)
- 361 Chen, K.H., Nadeau, R.M., Rau, R.: Characteristic repeating earthquakes in an arc-continent collision  
362 boundary zone: The Chihshang fault of eastern Taiwan. *Earth and Planetary Science Letters*.  
363 <https://doi.org/10.1016/j.epsl.2008.09.021> (2008)
- 364 Chetoni, R.: Terme di Prà di Lama (Pieve Fosciana, Lu), indagine geognostica sulle aree dissestate nel marzo  
365 1996. Geological Report. (1996)
- 366 [Cignetti, M., Manconi, A., Manunta, M., Giordan, D., De Luca, C., Allasia, P., Ardizzone, F.: Taking Advantage](#)  
367 [of the ESA G-POD Service to Study Ground Deformation Processes in High Mountain Areas: A Valle](#)  
368 [d’Aosta Case Study, Northern Italy. \*Remote Sensing\*, 8, 852. https://doi.org/10.3390/rs8100852 \(2016\)](#)
- 369 Closson, D.: Structural control of sinkholes and subsidence hazards along the Jordanian Dead Sea coast.  
370 *Environmental Geology*, 47 (2), 290-301. <https://doi.org/10.1007/s00254-004-1155-4> (2005)
- 371 Closson, D., Karaki, N.A., Klinger, Y., & Hussein, M. J.: Subsidence and Sinkhole Hazard Assessment in the  
372 Southern Dead Sea Area, Jordan. *Pure and Applied Geophysics*, 162, 221–248.  
373 <https://doi.org/10.1007/s00024-004-2598-y> (2005)
- 374 Rovida A., Locati M., Camassi R., Lolli B., Gasperini P.: CPTI15, the 2015 version of the Parametric Catalogue  
375 of Italian Earthquakes. Istituto Nazionale di Geofisica e Vulcanologia. [http://doi.org/10.6092/INGV.IT-](http://doi.org/10.6092/INGV.IT-CPTI15)  
376 [CPTI15](#) (2016)
- 377 De Luca, C., Cuccu, R., Elefante, S., Zinno, I., Manunta, M., Casola, V., Rivolta, G., Lanari, R., Casu, F.: An On-  
378 Demand Web Tool for the Unsupervised Retrieval of Earth’s Surface Deformation from SAR Data: The  
379 P-SBAS Service within the ESA G-POD Environment. *Remote Sensing*, 7(11), 15630-15650.  
380 <https://doi.org/10.3390/rs71115630> (2015)
- 381 De Stefani, C.: Le Acque Termali di Pieve Fosciana. *Memorie della Società Toscana di Scienze Naturali*, 4,  
382 72-97 (1879)
- 383 [Del Prete, S., Iovine, G., Parise, M., Santo, A.: Origin and distribution of different types of sinkholes in the](#)  
384 [plain areas of Southern Italy. \*Geodinamica Acta\* 23/1-3, 113-127. https://doi.org/10.3166/ga.23.113-](#)  
385 [127 \(2010\)](#)

- 386 Di Naccio, D., Boncio, P., Brozzetti, F., Pazzaglia, F. J., & Lavecchia, G.: Morphotectonic analysis of the  
387 Lunigiana and Garfagnana grabens (northern Apennines, Italy): Implications for active normal faulting.  
388 *Geomorphology*, 201, 293–311. <https://doi.org/10.1016/j.geomorph.2013.07.003> (2013)
- 389 Doglioni, C.: A proposal for the kinematic modelling of the W-dipping subduction – possible applications to  
390 the Tyrrhenian-Apennines system. *Terra Nova*, 3, 423-434. <https://doi.org/10.1111/j.1365-3121.1991.tb00172.x> (1991)
- 392 Elter, P., Giglia, G., Tongiorgi, M., Trevisan, L.: Tensional and compressional areas in the recent (Tortonian  
393 to Present) evolution of the Northern Apennines. *Bollettino di Geofisica Teorica ed Applicata*, 65 (8)  
394 (1975)
- 395 Faccenna, C. Florindo, F., Funicello, R., Lombardi, S.: Tectonic setting and Sinkhole Features: case histories  
396 from Western Central Italy. *Quaternary Proceedings*, 3, 47–56 (1993)
- 397 Faccenna, C. Becker, T.W., Miller, S.M., Serpelloni, E., & Willet, S.D.: Isostasy, dynamic topography, and the  
398 elevation of the Apennines of Italy. *Earth and Planetary Science Letters*, 407, 163–174.  
399 <https://doi.org/10.1016/j.epsl.2014.09.027> (1993)
- 400 Florea, L. J.: Using State-wide GIS data to identify the coincidence between sinkholes and geologic structure.  
401 *Journal of Cave and Karst Studies*, (August), 120–124. Retrieved from  
402 [http://digitalcommons.wku.edu/geog\\_fac\\_pub/14](http://digitalcommons.wku.edu/geog_fac_pub/14) (2005)
- 403 Ford, D.C., Williams, P., 2007.: Karst Hydrogeology and Geomorphology. *Wiley, Chichester*, (562 pp.)
- 404 Frumkin, A., & Raz, E.: Collapse and subsidence associated with salt karstification along the Dead Sea.  
405 *Carbonates and Evaporites*, 16(2), 117–130. <https://doi.org/https://doi.org/10.1007/bf03175830>  
406 (2001)
- 407 Giovannetti, F.: *Pieve Fosciana ieri e Oggi*. (1975)
- 408 [Gherardi, F., Pierotti, L.: The suitability of the Pieve Fosciana hydrothermal system \(Italy\) as a detection site  
409 for geochemical seismic precursors. \*Applied Geochemistry\*  
410 <https://doi.org/10.1016/j.apgeochem.2018.03.009> \(2018\)](https://doi.org/10.1016/j.apgeochem.2018.03.009)
- 411 [Gutiérrez, F., Guerrero, J., Lucha, P. A genetic classification of sinkholes illustrated from evaporite  
412 paleokarst exposures in Spain. \*Environmental Geology\*, 53. \[https://doi.org/10.1007/s00254-007-0727-  
413 5\]\(https://doi.org/10.1007/s00254-007-0727-5\) \(2008\)](https://doi.org/10.1007/s00254-007-0727-5)
- 414 [Gutiérrez, F., Parise, M., De Waele J., Jourde, H.: A review on natural and human-induced geohazards and  
415 impacts in karst. \*Earth-Science Reviews\*, 138. <https://doi.org/10.1016/j.earscirev.2014.08.002> \(2014\)](https://doi.org/10.1016/j.earscirev.2014.08.002)
- 416 Hanssen, R. F.: *Radar Interferometry: Data Interpretation and Error Analysis*. Kluwer Academic Publisher.  
417 <https://doi.org/10.1007/0-306-47633-9> (2001)
- 418 Harris, R.A.: Large earthquakes and creeping faults. *Reviews of Geophysics*, 55, 169-198.  
419 <https://doi.org/10.1002/2016RG000539> (2017)
- 420 Harrison, R. W., Newell, W. L., & Necdet, M.: Karstification Along an Active Fault Zone in Cyprus. Atlanta,  
421 Georgia. *U.S. Geological Survey Water-Resources Investigations Report 02-4174* (2002)
- 422 ISIDe working group version 1.0 (2016)

- 423 Johnson, A. G., Kovach, R. L., & Nur, A.: Pore pressure changes during creep events on the San Andreas  
424 Fault. *Journal of Geophysical Research*, 78 (5). <https://doi.org/10.1029/JB078i005p00851> (1973)
- 425 Kanamori, H.: The Energy Release in Great Earthquakes. *Journal of Geophysical Research*, 82(20).  
426 <https://doi.org/10.1029/JB082i020p02981> (1977)
- 427 [Kawashima, K., Aydan, O., Aoki, T., Kishimoto, I., Konagal, K., Matsui, T., Sakuta, J., Takahashi, N., Teodori,  
428 S.-P., Yashima, A.: Reconnaissance investigation on the damage of the 2009 L'Aquila, Central Italy  
429 earthquake. \*Journal of Earthquake Engineering\*. 14, 817–841.  
430 <https://doi.org/10.1080/13632460903584055> \(2010\)](https://doi.org/10.1080/13632460903584055)
- 431 Le Breton, E., Handy, M., Molli, G., & Ustaszewski K.: Post-20 Ma Motion of the Adriatic Plate: New  
432 Constraints from Surrounding Orogens and Implications for Crust-Mantle Decoupling. *Tectonics*, 36.  
433 <https://doi.org/10.1002/2016TC004443> (2000)
- 434 [Linde, A.T., Gladwin M.T., Johnston, M.J.S., Gwyther, R.L. and Bilham, R.G.: A slow earthquake sequence on  
435 the San Andreas fault. \*Nature\*, 383. <https://doi.org/10.1038/383065a0> \(1996\)](https://doi.org/10.1038/383065a0)
- 436 Manzo, M., Ricciardi, G.P., Casu F., Ventura, G., Zeni, G., Borgström S., Berardino, P., Del Gaudio, C., Lanari,  
437 R.: Surface deformation analysis in th Ischia Island (Italy) based on spaceborne radar interferometry.  
438 *Journal of Volcanology and Geothermal Research* 151, 399-416.  
439 <https://doi.org/10.1016/j.jvolgeores.2005.09.010> (2006)
- 440 Meletti, C., Patacca, E., & Scandone P.: Construction of a Seismotectonic Model: The Case of Italy. *Pure and  
441 applied Geophysics*, 157, 11-35. <https://doi.org/10.1007/PL00001089> (2000)
- 442 Micklethwaite, S., Sheldon, H. A., & Baker, T.: Active fault and shear processes and their implications for  
443 mineral deposit formation and discovery. *Journal of Structural Geology*, 32(2), 151–165.  
444 <https://doi.org/10.1016/j.jsg.2009.10.009> (2010)
- 445 Molli, G., Torelli, L., & Storti, F.: The 2013 Lunigiana (Central Italy) earthquake: Seismic source analysis from  
446 DInSar and seismological data, and geodynamic implications for the northern Apennines. A discussion.  
447 *Tectonophysics*, 668–669, 108–112. <http://dx.doi.org/10.1016/j.tecto.2015.07.041> (2016)
- 448  
449 Molli, G., Pinelli, G., Bigot, A., Bennett R., Malavieille J., Serpelloni E.: Active Faults in the inner northern  
450 Apennines: a multidisciplinary reappraisal. From 1997 to 2016: Three Destructive Earthquakes along  
451 the Central Apennine Fault system, Italy. July 19<sup>th</sup>-22<sup>nd</sup> 2017 Camerino, Volume Abstract (2017)
- 452 [Nadeau, R.M., Foxal, W., McEvelly, T.V.: Clustering and Periodic Recurrence of Microearthquakes on the San  
453 Andreas Fault at Parkfield, California. \*Science\*, 267. <https://doi.org/10.1126/science.267.5197.503>  
454 \(1995\)](https://doi.org/10.1126/science.267.5197.503)
- 455 Nayak, A., & Dreger, D. S.: Moment Tensor Inversion of Seismic Events Associated with the Sinkhole at  
456 Napoleonville Salt Dome, Louisiana. *Bullettin of the Seismological Society of America*, 104(4), 1763–  
457 1776. <https://doi.org/10.1785/0120130260> (2014)
- 458 Neuendorf, K., Mehl, J., Jackson, J.: Glossary of geology, 5th edn. *American Geological Institute*, 779 pp.  
459 (2005)
- 460 [Nishiguchi, T., Tsuchiya, S., Imaizumi, F.: Detection and accuracy of landslide movement by InSAR analysis  
461 using PALSAR-2 data. \*Landslides\*, 14:1483–1490. <https://doi.org/10.1007/s10346-017-0821-z> \(2017\)](https://doi.org/10.1007/s10346-017-0821-z)

- 462 Nisio, S.: The sinkholes in Tuscany Region. *Memorie Descrittive Carta Geologica d'Italia LXXXV* (2008)
- 463 Nof, R. N., Baer, G., Ziv, A., Raz, E., Atzori, S., & Salvi, S.: Sinkhole precursors along the Dead Sea, Israel,  
464 revealed by SAR interferometry. *Geology*, 41, (9), 1019-1022. <https://doi.org/10.1130/G34505.1>  
465 (2013)
- 466 Parise, M., Perrone, A., Violante, C., Stewart, J.P., Simonelli, A., Guzzetti, F.: Activity of the Italian National  
467 Research Council in the aftermath of the 6 April 2009 Abruzzo earthquake: the Sinizzo Lake case  
468 study. *Proc. 2nd Int. Workshop "Sinkholes in the Natural and Anthropogenic Environment", Rome, pp.*  
469 <http://doi.org/623-641>. 10.13140/2.1.3094.1127 (2010)
- 470 Parise, M. and Vennari, C.: A chronological catalogue of sinkholes in Italy: the first step toward a real  
471 evaluation of the sinkhole hazard. In: Land L, Doctor DH, Stephenson JB, editors. 2013. Sinkholes and  
472 the Engineering and Environmental Impacts of Karst: Proceedings of the Thirteenth Multidisciplinary  
473 Conference, May 6-10, Carlsbad, New Mexico: NCKRI Symposium 2. Carlsbad (NM): National Cave and  
474 Karst Research Institute. <http://doi.org/10.5038/9780979542275.1149> (2013)
- 475 Patacca, E., & Scandone, P.: Post-Tortonian mountain building in the Apennines, the role of the passive  
476 sinking of a relic lithospheric slab. *The Lithosphere in Italy*, 157–176 (1989)
- 477 Pepe, A. and Lanari, R. On the extension of the minimum cost flow algorithm for phase unwrapping of  
478 multitemporal differential SAR interferograms. *IEEE Transaction in Geoscience and Remote Sensing*,  
479 44, 9, 2374–2383. <http://doi.org/10.1109/TGRS.2006.873207> (2006)
- 480 Pezzo, G., Boncori, J.P.M., Atzori, S., Piccinini, D., Antonioli, A., Salvi, S.: The 2013 Lunigiana (Central Italy)  
481 earthquake: Seismic source analysis from DInSAR and seismological data, and geodynamical  
482 implications for the northern Apennines. *Tectonophysics* 636, 315–324.  
483 <http://dx.doi.org/10.1016/j.tecto.2014.09.005>. (2014)  
484
- 485 Pinelli, G.: Tettonica recente e attiva nell'Appennino interno a Nord dell'Arno: una revisione delle strutture  
486 e delle problematiche. Diploma Thesis (89 pp) (2013)
- 487 Raffaelli, R.: Sulle acque termali di Pieve Fosciana (1869)
- 488 Rau, R., Chen, K.H., Ching, K.: Repeating earthquakes and seismic potential along the northern Longitudinal  
489 Valley fault of Taiwan. *Geophysical Research Letters*, 34. <http://doi.org/10.1029/2007GL031622>  
490 (2007)
- 491 Rovida A., Locati M., Camassi R., Lolli B., Gasperini P.: CPTI15, the 2015 version of the Parametric Catalogue  
492 of Italian Earthquakes. *Istituto Nazionale di Geofisica e Vulcanologia*. [http://doi.org/10.6092/INGV.IT-](http://doi.org/10.6092/INGV.IT-CPTI15)  
493 [CPTI15](http://doi.org/10.6092/INGV.IT-CPTI15) (2016)
- 494 Salamon, A.: Seismically induced ground effects of the February 11, 2004, M L = 5.2, North-eastern Dead  
495 Sea earthquake. *Geological Survey of Israel Report* (2004)
- 496 Santo, A., Del Prete, S., Di Crescenzo, G., and Rotella M.: Karst processes and slope instability: some  
497 investigations in the carbonate Apennine of Campania (southern Italy). In: Parise, M., Gunn, J. (Eds.),  
498 Natural and Anthropogenic Hazards in Karst Areas: Recognition, Analysis, and Mitigation. *Geological*  
499 *Society, London*, 279, pp. 59–72. <http://doi.org/10.1144/SP279.60305-8719/07> (2007)
- 500 Serpelloni, E., Anzidei, M., Baldi, P., Casula, G., & Galvani, A.: Crustal velocity and strain -rate fields in Italy  
501 and surrounding regions: New results from the analysis of permanent and non-permanent GPS

502 networks. *Geophysical Journal International*, 161(3), 861–880. [https://doi.org/10.1111/j.1365-](https://doi.org/10.1111/j.1365-246X.2005.02618.x)  
503 [246X.2005.02618.x](https://doi.org/10.1111/j.1365-246X.2005.02618.x) (2005)

504 Shalev, E., & Lyakhovsky, V.: Viscoelastic damage modeling of sinkhole formation. *Journal of Structural*  
505 *Geology*, 42, 163–170. <https://doi.org/10.1016/j.jsg.2012.05.010> (2012)

506 Scholz, C. H.: Earthquakes and friction laws. *Nature*, 391, 37–42. <https://doi.org/10.1038/34097> (1998)

507 Sibson, R. H.: Roughness at the Base of the Seismogenic Zone: Contributing Factors. *Journal of Geophysical*  
508 *Research*, 87 (B7), 5791-5799. <https://doi.org/10.1029/JB089iB07p05791> (1984)

509 Sibson, R. H.: Structural permeability of fluid-driven fault-fracture meshes. *Journal of Structural Geology*, 18  
510 (8),1031-1042. [https://doi.org/10.1016/0191-8141\(96\)00032-6](https://doi.org/10.1016/0191-8141(96)00032-6) (1996)

511 Stramondo, S., Vannoli, P., Cannelli, V., Polcari, M., Melini, D., Samsonov, S., Moro, M., Bignami, C., & Saroli,  
512 M.: X- and C-band SAR surface displacement for the 2013 Lunigiana earthquake (Northern Italy): a  
513 breached relay ramp? *IEEE J. Sel. Top. Appl. Earth Obs. Remote Sens.*  
514 <http://dx.doi.org/10.1109/JSTARS.2014.2313640> (2014)

515 Tertulliani, A., & Maramai, A.: Macroseismic evidence and site effects for the Lunigiana (Italy) 1995  
516 Earthquake. *Journal of Seismology*, 2 (3), 209–222. <https://doi.org/10.1023/A:1009734620985> (1998)

517 Vannoli, P.: Il terremoto in Garfagnana del 25 gennaio 2013 visto dal geologo. Retrieved from  
518 [https://ingvterremoti.wordpress.com/2013/02/06/il-terremoto-del-25-gennaio-2013-visto-dal-](https://ingvterremoti.wordpress.com/2013/02/06/il-terremoto-del-25-gennaio-2013-visto-dal-geologo/#more-3132)  
519 [geologo/#more-3132](https://ingvterremoti.wordpress.com/2013/02/06/il-terremoto-del-25-gennaio-2013-visto-dal-geologo/#more-3132) (2013)

520 Wadas, S. H., Tanner, D. C., Polom, U., & Krawczyk, C. M.: Structural analysis of S-wave seismics around an  
521 urban sinkhole; evidence of enhanced suberosion in a strike-slip fault zone. *Natural Hazards and Earth*  
522 *System Sciences*. <https://doi.org/10.5194/nhess-2017-315> (2017)

523 Wei, M., Sandwell, D., & Fialko, Y.: A silent Mw 4.7 slip event of October 2006 on the Superstition Hills fault,  
524 southern California. *Journal of Geophysical Research*, 114, B07402,  
525 <https://doi.org/10.1029/2008JB006135> (2009)

526 Yarushina, V. M., Podladchikov, Y.Y., Minakov, A., & Räss, L.: On the Mechanisms of Stress-Triggered  
527 Seismic Events during Fluid Injection. *Sixth Biot Conference on Poromechanics, American Society of*  
528 *Civil Engineers*. <https://doi.org/10.1061/9780784480779.098> (2017)

529

530

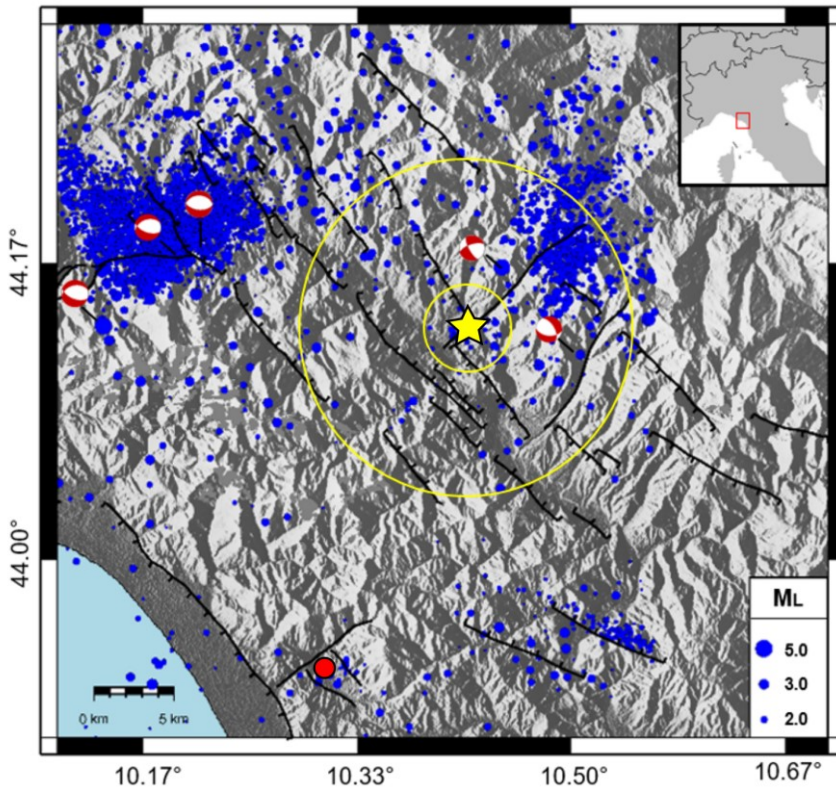
531

532

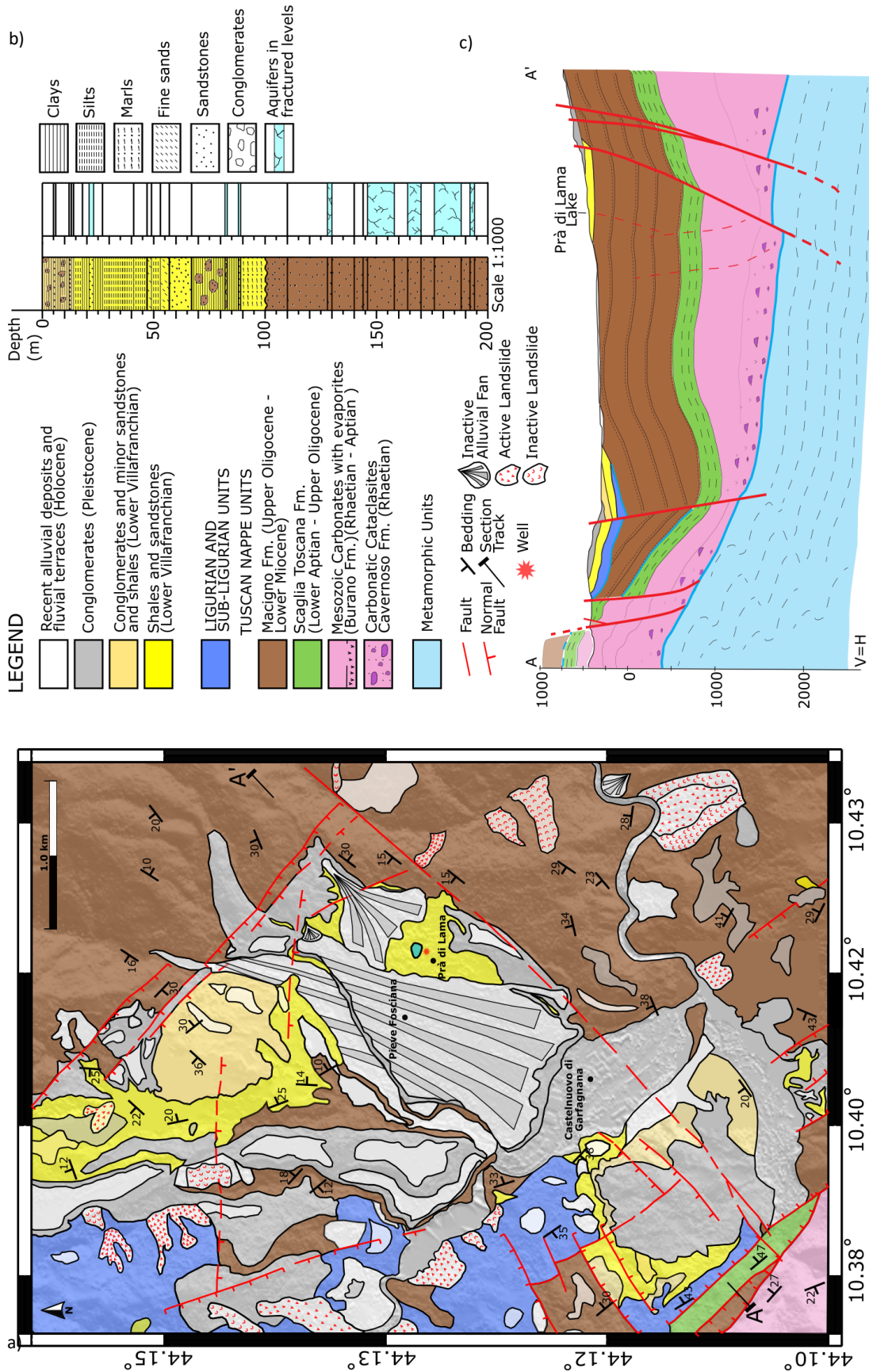
533

534

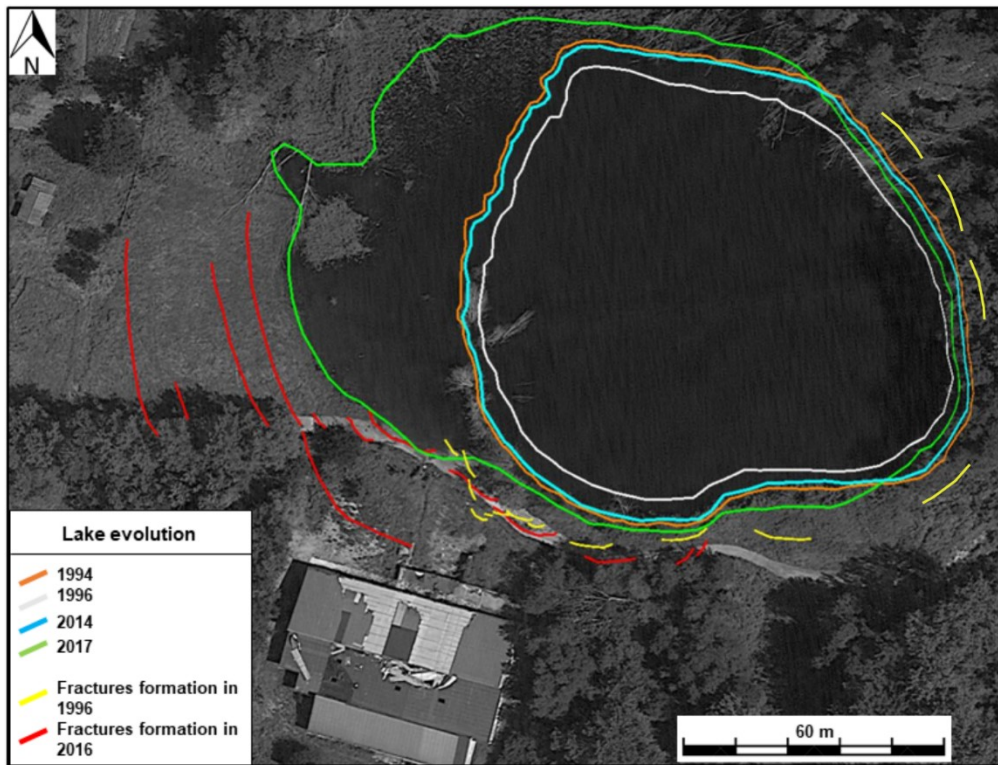
535



548 **Figure 1 - Study area.** The Pieve FosciianaPrà di Lama sinkhole-area is marked by the red dotyellow star. Black tick lines are faults.  
 549 Blue dots are the earthquakes between 1986 and 2017. Focal mechanisms are from the Regional Centroid Moment Tensor (RCMT)  
 550 catalogue. The yellow circles represent the areas with radii of 3km and 10 km used for the seismicity analysis. The red dot is the  
 551 sinkhole of Camaiore (Caramanna et al. 2008). The red box in the *inset* marks the location of the area shown in the main figure.  
 552  
 553

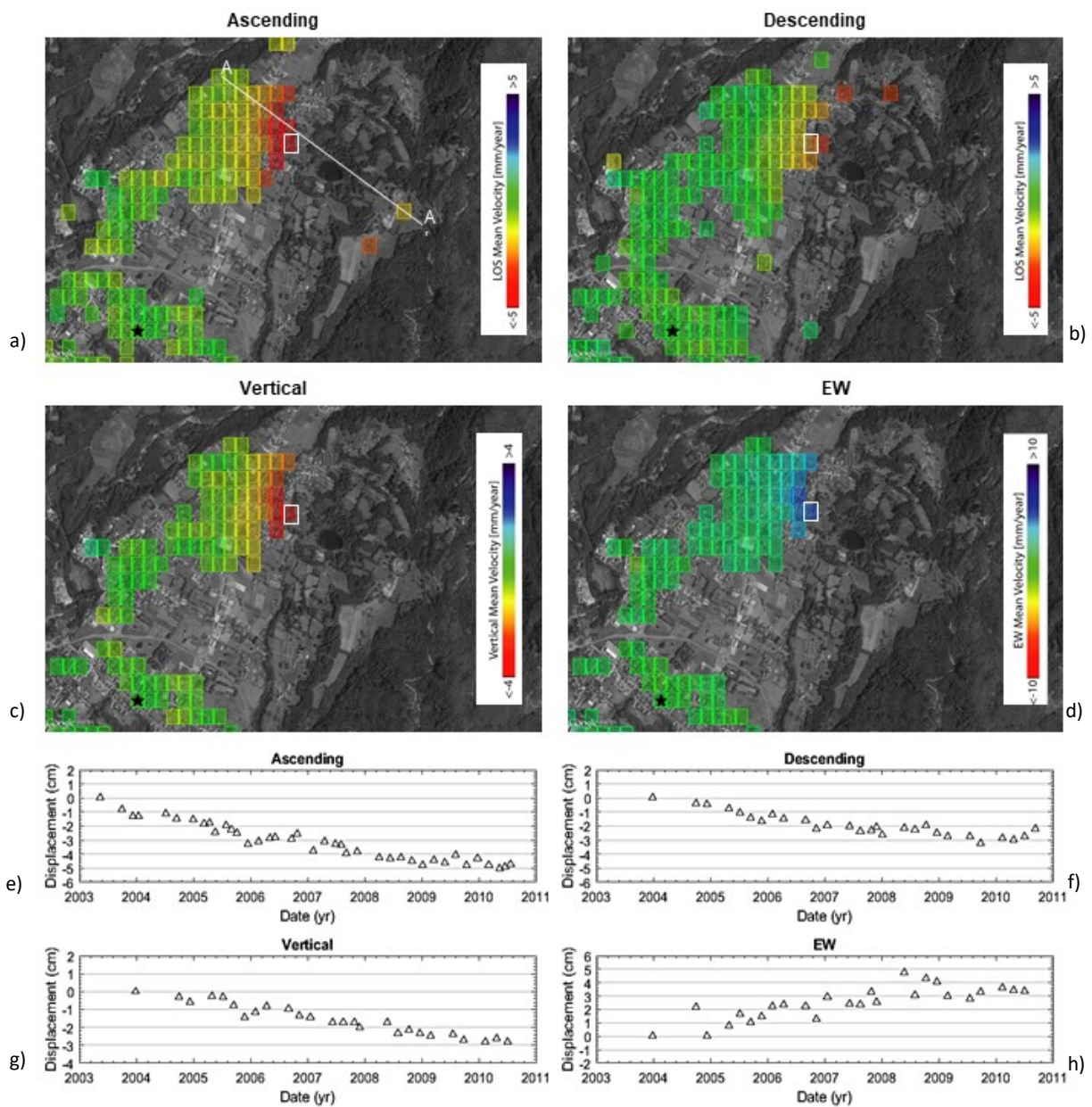


554 **Figure 2 – Geological setting of the study area. a)** Geological, structural and geomorphological map of the area nearby Prà di Lama  
 555 **showing the main tectonic and lithostratigraphic units. b)** Schematic sedimentary sequence of the Villafranchian deposits obtained  
 556 **from the well drilled at Prà di Lama (Modified from Chetoni 1995). c)** Stratigraphic cross-section across the Garfagnana graben.



557  
558  
559

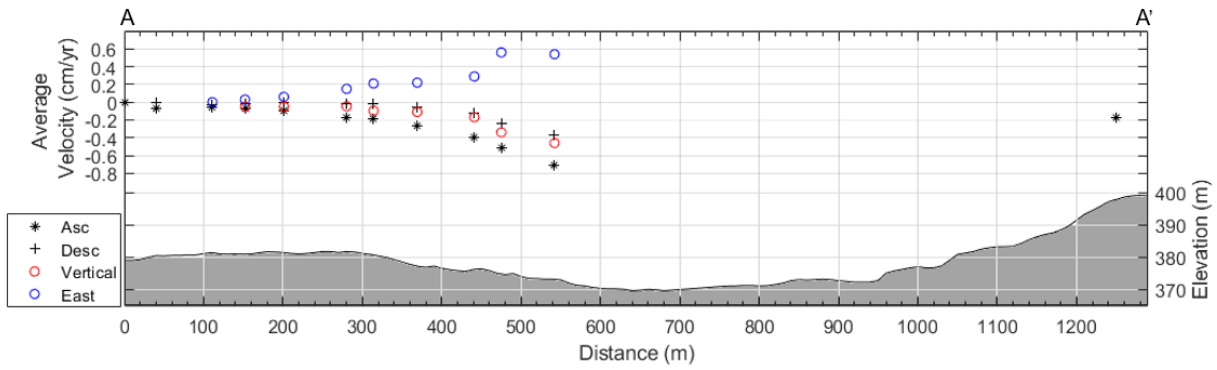
**Figure 3 – Evolution of the Prà di Lama lake between 1994 and 2017.** Lake shores variation have been retrieved from the analysis of Landsat image



560  
561

562 **Figure 4 – a, b** Maps of average surface velocity and its vertical **(c)** and East-West **(d)** components obtained from ENVISAT SAR  
563 images acquired between 2003 and 2010. Negative values indicate range increase. The white line in panel a) marks the cross-  
564 section shown in figure 4. The black star is the point used as reference for the InSAR-SBAS processing. **e, f, g, h** Time-series of  
565 incremental deformation extracted from the pixel bounded with the white rectangle.

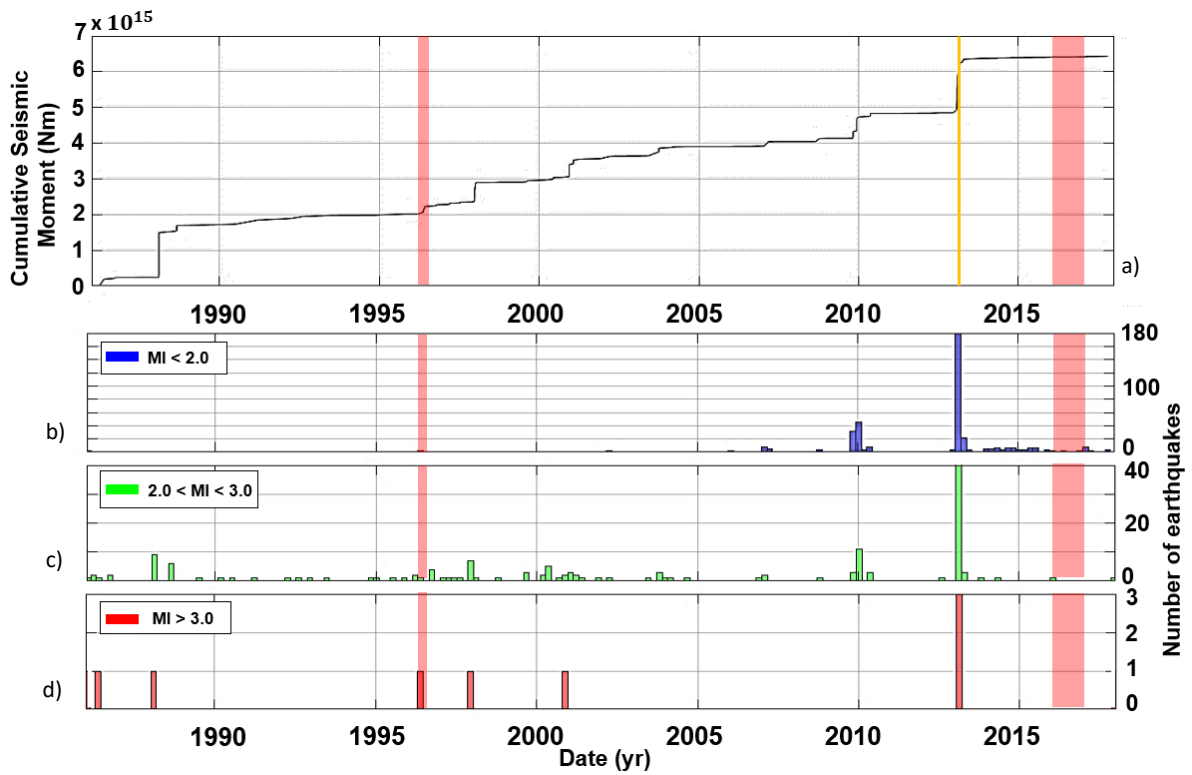
566



567

568 **Figure 5 - Cross-section of topography and InSAR velocities along the A-A' profile as shown in figure 3a.**

569

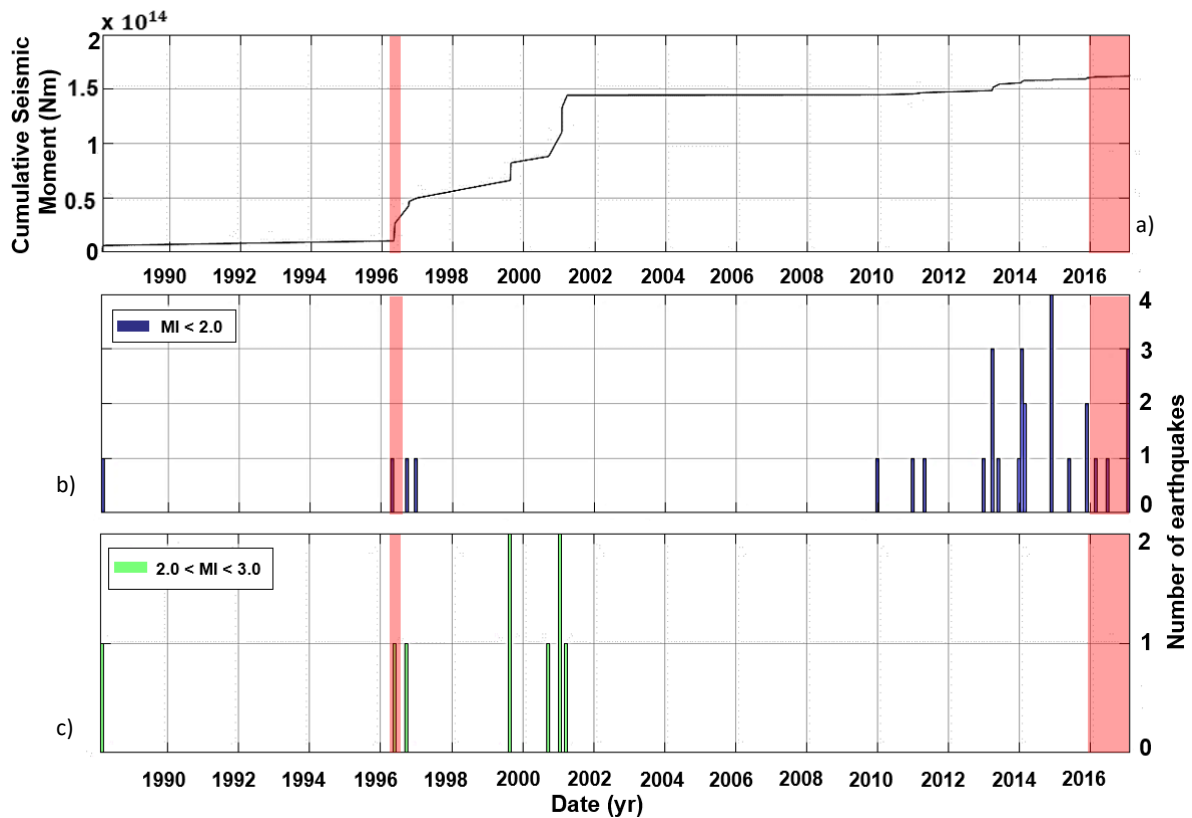


570

571 **Figure 6 – Seismicity features of an area 10 km in radius around the Prà di Lama lake.** cumulative seismic moment released in the  
 572 area (a) and histograms of the number of earthquakes per month. Three different classes of magnitude have been created: MI < 2.0  
 573 (b), 2.0 < MI < 3.0 (c) and MI > 3.0 (d). The dataset covers the period between 1986 and 2017. The red transparent bars indicate the  
 574 two events of unrest of 1996 and 2016.

575

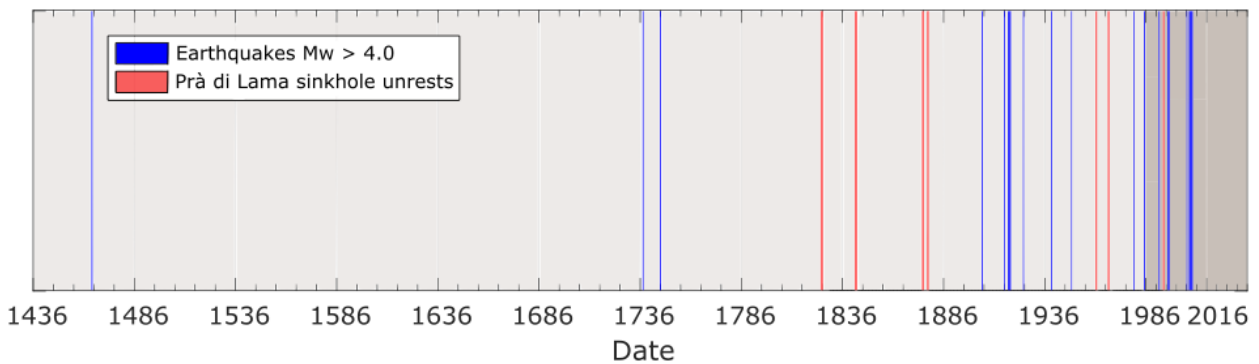
576



577  
578  
579  
580  
581

**Figure 7 - Seismicity features of an area 3 km in radius around the Prà di Lama lake.** Plot of the cumulative seismic moment released in the area (a) and histograms showing the number of earthquakes occurred each month. Two different classes of Magnitude have been created:  $M_I < 2.0$  (b),  $2.0 < M_I < 3.0$  (c). No events of  $M_I > 3.0$  occurred in the area between 1986 and 2017. The red transparent bars indicate the two events of unrest of 1996 and 2016.

582  
583



584  
585

**Figure 8 – Comparison between the earthquakes (blue lines) in the Garfagnana area (INGV Catalogo Parametrico dei Terremoti Italiani CPT15, Rovida et al., 2016), and events of unrest at the Prà di Lama sinkhole (red lines).**

586  
587  
588  
589

| <b>Year</b>      | <b>Brief description of the event</b>   |
|------------------|---|
| <b>991</b>       | Seasonal pool fed by springs  |
| <b>1828</b>      | Bursts of the springs water flow. Uprising of muddy waters and clays ( <i>Raffaelli, 1869; De Stefani, 1879</i> )           |
| <b>1843</b>      | Bursts of the springs water flow. Uprising of muddy waters and clays ( <i>Raffaelli, 1869; De Stefani, 1879</i> )           |
| <b>1876</b>      | Subsidence and fracturing ( <i>De Stefani, 1879</i> )   |
| <b>1877</b>      | Subsidence and fracturing ( <i>De Stefani, 1879</i> )   |
| <b>1962</b>      | Bursts of the spring water flow. Uprising of muddy waters and clays ( <i>Giovannetti, 1975</i> )                            |
| <b>1969</b>      | Abrupt falling of the water level and fracturing along the shores. The lake almost disappeared ( <i>Giovannetti, 1975</i> ) |
| <b>1985</b>      | Arising of muddy waters in a well   |
| <b>1996</b>      | Abrupt fall of the water level and fracturing along the shores  |
| <b>2016-2017</b> | Subsidence and fracturing   |

591 *Table 1 – Description of the activity at Prà di Lama lake*